Transcriptomic analysis reveals immune signatures associated with specific cutaneous manifestations of lupus in systemic lupus erythematosus

Ernest Y. Lee[1,4,5], Sarah Patterson[2], Zachary Cutts[4,5], Cristina M. Lanata[6], Maria Dall'Era[2], Jinoos Yazdany[2], Lindsey A. Criswell[6], Anna Haemel[1], Patricia Katz[2], Chun Jimmie Ye[2], Charles Langelier[3], Marina Sirota[4,5*]

[1] Department of Dermatology, University of California, San Francisco, San Francisco, CA, United States

[2] Division of Rheumatology, Department of Medicine, University of California, San Francisco, San Francisco, CA, United States

[3] Division of Infectious Diseases, Department of Medicine, University of California, San Francisco, San Francisco, CA, United States

[4] Department of Pediatrics, University of California, San Francisco, San Francisco, CA, United States

[5] Bakar Computational Health Sciences Institute, University of California, San Francisco, San Francisco, CA, United States

[6] Genomics of Autoimmune Rheumatic Disease Section, National Human Genome Research Institute, National Institutes of Health, Bethesda, MD, United States.

*Corresponding Authors:

Marina Sirota (marina.sirota@ucsf.edu)

23 Bakar Computational Health Sciences Institute, University of California, San Francisco, San
24 Francisco, CA, United States
25

26 **Abstract**

27 Systemic lupus erythematosus (SLE) presents with diverse heterogenous cutaneous
28 manifestations. However, the molecular and immunologic pathways driving specific cutaneous
29 manifestations of SLE are poorly understood. Here, we leverage transcriptomics from a large
30 well-phenotyped longitudinal cohort of SLE patients to map molecular pathways linked to ten
31 distinct SLE-related rashes. Through whole blood and immune cell-sorted bulk RNA sequencing,
32 we identified immune signatures specific to cutaneous subtypes of SLE. Subacute cutaneous
33 lupus (SCLE) exhibited broad upregulation of interferon, TNF-α, and IL6-JAK-STAT3 pathways
34 suggesting potential unique therapeutic responses to JAK and type I interferon inhibition. While
35 interferon signaling is prominent in SCLE, discoid lupus, and acute lupus, it is unexpectedly
36 attenuated in patients with skin and mucosal ulcers. Pathway and cell-type enrichment analysis
37 revealed unexpected roles for CD14+ monocytes in photosensitivity of SLE and NK cells in
38 alopecia, mucosal ulceration, and livedo reticularis. These findings illuminate the immune
39 heterogeneity of rashes in SLE, highlighting subtype-specific mechanistic targets, and
40 presenting opportunities for precision therapies for SLE-associated skin phenotypes.

41 **Introduction**

42 Systemic lupus erythematosus (SLE) is a chronic autoimmune inflammatory disorder
43 characterized by broad and heterogenous clinical manifestations that reflect complex,
44 dysregulated immune responses (1). Cutaneous lupus erythematosus (CLE) encompasses
45 various mucocutaneous manifestations, including acute cutaneous lupus (ACLE, includes malar
46 rash), chronic cutaneous lupus erythematosus (CCLE, includes discoid lupus and chilblain lupus),
47 subacute cutaneous lupus erythematosus (SCLE), and lupus panniculitis. However, lupus also
48 manifests clinically as alopecia, skin and mucosal ulcers, and livedo reticularis (2, 3). A large
49 subset of patients with SLE will exhibit cutaneous lupus, though not all patients with cutaneous
50 lupus will progress to SLE(4). These distinct cutaneous manifestations not only contribute to
51 disease burden but also hint at underlying immunological heterogeneity, suggesting that
52 different pathways may drive specific phenotypes. Despite advances in our understanding of
53 SLE immunopathology, the immune drivers of specific SLE-related cutaneous manifestations
54 amongst patients with SLE remain poorly understood.

55 At present, we are unable to predict or identify which patients with SLE will exhibit
56 specific cutaneous manifestations. Although a subset of SLE patients will initially present with a
57 rash, many patients may initially present with lupus nephritis or neurologic symptoms.
58 Although malar rash and discoid rash are part of the classification criteria for SLE, we now
59 recognize that there are other cutaneous manifestations of SLE, not part of the classification
60 criteria, that have significant clinical and psychosocial impacts on SLE patients (2, 5). Since SLE is
61 an immunologically complex disorder, identifying molecular pathways that are associated with

62 specific SLE-related cutaneous lesions and illuminating new molecular targets is of utmost
63 clinical importance.

64 High-throughput transcriptomic profiling has proven valuable in mapping immune
65 dysregulation in autoimmune diseases and identifying disease-specific clinically relevant gene
66 signatures across many autoimmune and inflammatory conditions including SLE (6–11). To
67 study the SLE disease heterogeneity, identify biomarkers and discover therapeutic targets,
68 several studies have utilized bulk RNA sequencing (bulk RNAseq) of whole blood (8), as well as
69 single-cell RNA sequencing (scRNAseq) of peripheral blood mononuclear cells (PBMCs) (12) to
70 identify specific gene signatures in cell types crucial to lupus pathogenesis. In addition, they
71 have identified key gene signatures related to type I interferon signaling in B cells, plasma cells,
72 and granulocytes in SLE (13–15). Prior work also has showed how the American College of
73 Rheumatology (ACR) classification criteria of SLE clusters into subgroups that are related to
74 specific differences in clinical phenotypes and lupus severity (16)(17), and identified race-
75 specific and cell-type specific immunologic differences in clinical clusters of SLE patients (18).
76 Transcriptomic analysis previously identified differentially expressed transposable elements
77 across all phenotypes that were cell-type and phenotype specific, and were related to genes
78 primarily involved in antiviral signaling and IFN signaling (19). Methylation analysis of SLE
79 patients identified 256 differentially methylated CpGs across disease associated with ethnic-
80 associated clinical outcomes (16). Several prior studies have also utilized bulk RNAseq and
81 scRNAseq on skin biopsies from healthy patients and SLE patients with discoid lupus or acute
82 cutaneous lupus to identify a role for infiltration of plasmacytoid dendritic cells and
83 upregulation of an associated type I interferon signature in cutaneous lesions (20–23). These

84 previous studies focused primarily on differentiating SLE patients from healthy controls and
85 identifying gene signatures in whole blood related to global disease activity and cytokine
86 profiles, and clinical manifestations such as lupus nephritis. However, few studies have focused
87 on identifying immunologic pathways in the blood that are predictive of cutaneous phenotypes,
88 and none have a large enough sample size to encompass the entire clinical spectrum of SLE-
89 related cutaneous manifestations. Furthermore, these studies are often limited to smaller
90 cohorts with more homogeneous and less diverse demographics, limiting the predictive power
91 and generalizability.

92 Leveraging a large, high-quality ethnically diverse longitudinal cohort of >400 SLE
93 patients with carefully curated clinical data from the California Lupus Epidemiology Study
94 (CLUES), we identify molecular correlates associated with specific cutaneous features of lupus.
95 Through parallel whole blood and immune cell-sorted bulk RNA sequencing, we describe
96 transcriptional profiles across ten distinct subtypes of SLE-related rashes, enabling us to
97 characterize immune pathways and cellular contributors with unprecedented specificity. Our
98 findings reveal a diverse landscape of immune signatures underlying subtypes of SLE-related
99 cutaneous manifestations.

100

101 **Results**

102

103 **Transcriptomic landscape of cutaneous manifestations of SLE in the CLUES cohort**

104 Participants were recruited from the California Lupus Epidemiology Study (CLUES).
105 CLUES is a multi-racial/ethnic cohort of patients with confirmed SLE (Figure 1). SLE diagnosis

106 was confirmed by board certified study physicians based on the ACR revised criteria from 1982
107 and updated in 1997 or based upon a confirmed diagnosis of lupus nephritis. These patients
108 were longitudinally followed from time of enrollment with careful annotation of clinical
109 characteristics and molecular measurements (Figure S1). In this study, we focused on 10
110 different rashes and/or cutaneous manifestations related to SLE: acute cutaneous lupus (malar
111 rash), discoid lupus (DLE), photosensitivity, mucosal ulcers, skin ulcers, alopecia, subacute
112 cutaneous lupus (SCLE), lupus panniculitis, livedo reticularis, and other rashes related to SLE
113 (Figure 1). We excluded other clinical phenotypes due to low incidence. We generated two
114 datasets to be analyzed together. Bulk RNA sequencing of whole blood was conducted on N =
115 461 samples taken from 276 CLUES patients. The CLUES cohort represents both female and
116 male patients, though is majority female, across eight different self-reported races spanning a
117 range of low to high lupus severity as measured by standardized clinical criteria (lupus severity
118 index) (Table 1). We also evaluated a subset of N = 120 samples from SLE patients with cell-
119 sorted bulk RNA sequencing of CD4+ T cells, CD14+ monocytes, B cells, and NK cells (Figure 1).
120 After quality control (Figure S2) and comprehensive analysis of the clinical metadata to
121 identify specific dermatologic manifestations of lupus, we then conducted differential gene
122 expression, pathway analysis, and cell-type enrichment on each clinical phenotype to identify
123 transcriptomic and immunologic signatures associated with SLE related rashes (Figure 1). The
124 CLUES cohort represents both female and male patients, though is majority female, across eight
125 different self-reported races spanning a range of low to high lupus severity as measured by
126 standardized clinical criteria (SLE disease activity index (SLEDAI) score and lupus severity index).
127 Most patients in this cohort had a history of malar rash, mucosal ulcers, photosensitivity, and

128 alopecia, with a smaller subset of patients with DLE or SCLE (Figure 2A). Lupus panniculitis, skin
129 ulcers, livedo reticularis were less common. Principal component analysis (PCA) plots of the
130 overall bulk transcriptomic data from whole blood for subpopulations of patients with each of
131 the different SLE-related rashes are shown (Figure 2B, Figure S3). In the first two principal
132 components, there is no clear separation or clustering of the clinical subsets of the patients
133 with or without a specific SLE-related rash, suggesting that more subtle molecular effects may
134 be responsible for different clinical findings. No significant batch effect is seen with the two
135 runs of samples being collected in parallel. All annotated phenotypes of SLE-related cutaneous
136 manifestations are shown together with the raw dataset of bulk RNAseq counts across all
137 samples (Figure S4).
138
139 **Interactome and disease signatures of distinct SLE-related rashes**
140 To further identify molecular differences underlying SLE-related rashes, we conducted
141 differential gene expression analyses with Deseq2 (24). First, we conducted differential
142 expression on the whole blood transcriptomes for each clinical phenotype while controlling for
143 demographic features and clinical parameters such as sex, race, medication use, replicates, and
144 batch, and then compared our findings to the differential gene expression on the cell-sorted
145 bulk transcriptomes from CD4 T cells, CD14 monocytes, CD19 B cells, and NK cells. For each
146 differential gene expression analysis, we compared patients with and without specific
147 cutaneous manifestations of lupus. There were 2 differentially expressed genes (DEGs) (FDR <
148 0.05) in the blood of patients with discoid lupus, 6 DEGs in patients with alopecia, 4 DEGs in
149 SCLE, 1 DEGs in malar rash, 2 DEGs in livedo, 6 DEG in skin ulcers, 4 DEGs for mucosal ulcers,

150 and 2 DEGs for photosensitivity (Table 2). 8 DEGs were identified for lupus panniculitis. Utilizing
151 the identities of these genes, we were able to generate an interactome of SLE-related rashes
152 based on shared DEGs between each pairwise combination of cutaneous phenotypes (Figure
153 3A, Figure S5A). We then calculated the log-2-fold-change (log2FC) for the union of each of the
154 identified DEGs (34 total unique genes) from all clinical phenotypes across whole blood to
155 visualize the differential expression fingerprint for each gene. Hierarchical clustering of these
156 manifestations shows similarities between the expression fingerprints of lupus panniculitis, skin
157 ulcers, and SCLE (Figure 3A).

158 Since comparatively fewer differentially expressed genes were identified from the
159 whole blood RNAseq, we then conducted differential gene expression on each SLE-related rash
160 for the bulk transcriptomes from sorted immune cells from a subset of the CLUES cohort. We
161 looked at differential gene expression in CD4 T cells, CD14 monocytes, CD19 B cells, and NK
162 cells, to identify cell-type specific gene signatures for each cutaneous clinical phenotype of
163 interest. We then plotted the log2FC for the union of all DEGs for each cell type across
164 phenotypes. The expression fingerprints of all DEGs in the CD4 T-cells (821 total genes) were
165 plotted for all clinical phenotypes (Figure 3B). In CD4 T-cells, livedo reticularis and SCLE shared
166 238 DEGs, while 3 DEGs were shared between livedo and mucosal ulcers, 2 DEGs shared
167 between malar rash and SCLE, and 1 gene shared between SCLE and skin ulcers (Figure 3B,
168 Figure S5B). Most of the DEGs identified in the CD4 cohort were upregulated genes.
169 Hierarchical clustering of the clinical phenotypes showed similarity between patients with skin
170 ulcers and lupus panniculitis, while SCLE and livedo were also closely similar, given the large
171 number of shared DEGs.

172 In the CD14 monocytes, surprisingly we identified 14 common DEGs between the malar
173 rash and skin ulcer phenotypes, and less than 4 shared DEGs between patients with
174 photosensitivity, mucosal ulcers, and alopecia (Figure 3C, Figure S5C). Expression fingerprints of
175 all DEGs (589 total genes) in CD14 cells showed closer similarity between patients with skin
176 ulcers and panniculitis, but opposite gene expression patterns between malar rash and skin
177 ulcers (Figure 3C). In the CD19 B cells, the gene expression fingerprints of all DEGs in the CD19
178 cells (383 total genes) showed significant similarity between SCLE and panniculitis with
179 hierarchical clustering. The most DEGs in common were identified between SCLE and
180 panniculitis, SCLE and photosensitivity, and panniculitis and photosensitivity (Figure 3D, Figure
181 S5D). There were 47 DEGs shared between SCLE and panniculitis, 17 shared between SCLE and
182 photosensitivity. Finally, in the NK cells, the clinical phenotypes clustered separately based on
183 shared DEGs. Fewer total DEGs were seen across all phenotypes (72 total genes) compared to
184 the CD4, CD14, and CD19 cell types (Figure 3E, Figure S5E). Very few DEGs were shared
185 between clinical phenotypes, compared to larger overlaps in the other cell types. Only 3 shared
186 DEGs were identified for alopecia and malar rash, 2 DEGs for skin ulcers and livedo, and 1 DEG
187 for other phenotypes.
188
189 **Global and cell-type specific immunologic pathways dysregulated in cutaneous phenotypes of**
190 **SLE**
191 Next, we asked which molecular pathways are dysregulated in the whole blood of
192 patients with cutaneous manifestations of lupus. We calculated the differential gene expression
193 profiles from Deseq2 for each cutaneous phenotype and conducted gene set enrichment

194 analysis using FGSEA (25). We utilized the Hallmark pathways from MSigDB (26) for each SLE-
195 related rash. We identified several significant upregulated and downregulated pathways for
196 each SLE-related rash in whole blood (padj < 0.05) (Figure 4A, Figure S6).

197 In whole blood, interferon alpha and interferon gamma response were globally
198 upregulated across patients with discoid rash, alopecia, SCLE, livedo, and lupus panniculitis
199 (Figure 4A). Surprisingly, interferon alpha and gamma pathways were downregulated in
200 patients with skin ulcers and mucosal ulcers, potentially suggesting that type I interferon does
201 not directly drive these clinical sub-phenotypes. From hierarchical clustering, SCLE and lupus
202 panniculitis clustered together in terms of pathway signatures. We also observed that the
203 pathway signatures more closely clustered for malar rash, discoid rash, livedo, and alopecia.
204 Separately, we identified that activation of the heme metabolism pathway was the strongest in
205 patients with alopecia. Lupus panniculitis exhibited upregulation of interferon response
206 pathways, it exhibits downregulation of heme metabolism, TNF signaling, and UV response
207 pathways.

208 Now that we identified global pathway signatures for each clinical phenotypes, we
209 asked whether pathways detected in specific SLE-related rashes were specific to certain cell
210 types. More specifically, we carried out similar differential gene expression analyses for CD4,
211 CD14, CD19, and NK cells (Figure 4B-E). CD4 T cells exhibited upregulation in IFN alpha and
212 gamma related pathways across several phenotypes including malar rash, discoid rash, SCLE,
213 panniculitis, and photosensitivity (Figure 4B). The mammalian target of rapamycin (mTOR)
214 pathway which is relevant to CD4 T cell activation and proliferation was also upregulated.
215 Numerous pathways related to metabolism and cellular respiration and turnover was also

216 upregulated. Interestingly, TNF pathway activation was only seen in a smaller subset of
217 phenotypes, including SCLE, alopecia, and livedo reticularis, but not in malar rash or discoid
218 lupus. The JAK/STAT pathways related to IL2 and IL6 were more strongly prominent in livedo,
219 alopecia, and photosensitivity, which clustered together with hierarchical clustering.

220 CD14 monocytes and macrophages are known to be dysregulated in SLE, but their role
221 in development of cutaneous lupus is poorly understood. Previous studies have shown that
222 monocytes in SLE exhibit defective phagocytosis as well as aberrant activation in disease
223 initiation and mediation of end organ damage (27). Globally, CD14 monocytes exhibit varied
224 differential pathway expression across cutaneous phenotypes. Interferon alpha and gamma
225 pathways were upregulated in malar rash, discoid rash, SCLE, and photosensitivity. Across all
226 pathways, malar and discoid rash clustered together along with mucosal ulcers, while SCLE,
227 photosensitivity, and alopecia clustered together (Figure 4C). Surprisingly, TNF signaling was
228 upregulated in SCLE, lupus panniculitis, and photosensitivity, but downregulated across malar
229 and discoid rash, and mucosal ulcers. CD14 monocytes also exhibited significant expression of
230 downregulated UV response pathways in SCLE and photosensitivity, suggesting that they are
231 involved in regulating immune responses to UV radiation in those conditions.

232 CD19 B cells exhibited the broadest number of upregulated proinflammatory pathways
233 of all the cell types studied. It is well known that B cells play a central role in the pathogenesis
234 of SLE. Across most clinical phenotypes, type I interferon signaling was upregulated, as well as
235 the JAK-STAT pathways related to IL2 and IL6 signaling, complement cascade, and TNF signaling
236 (Figure 4D). In particular, the IL6/JAK/STAT3 pathway was prominently upregulated in acute
237 cutaneous lupus (malar rash), discoid lupus, and SCLE. They also exhibited strong and significant

238 upregulation of complement pathways and the IL6/JAK-STAT3 pathways alongside the
239 interferon pathways. Significant activation of the IL2/STAT5 pathway, which also involves
240 JAK1/JAK3, were also seen in malar rash, SCLE, and lupus panniculitis. This suggests a potential
241 supplemental role for JAK signaling in a subset of SLE patients with SCLE and discoid lupus. The
242 CD19 B cell compartment also showed a high degree of metabolic activity and cell turnover,
243 suggesting high proliferation rate. As expected, photosensitive conditions such as SCLE, malar
244 rash, and photosensitivity showed upregulation of the UV response pathways. Hierarchical
245 clustering identified three sub-clusters of clinical phenotypes within the CD19 compartment. In
246 particular, the pathway signatures were similar between alopecia, photosensitivity, malar rash,
247 and mucosal ulcers. Separately, discoid lupus, SCLE, and lupus panniculitis clustered together. In
248 contrast, livedo reticularis and skin ulcers exhibit fewer upregulated inflammatory pathways.
249 In the NK cell compartment, we observed fewer differentially expressed genes and
250 fewer significantly enriched pathways overall. However, upregulated NK cell pathways appear
251 to play a role in alopecia, skin and mucosal ulcers, discoid lupus, and livedo, but to a lesser
252 degree in malar rash or photosensitivity (Figure 4E). From hierarchical clustering, we identify
253 mucosal ulcers and alopecia with similar pathway signatures in NK cells, with upregulation of
254 pathways related to cellular metabolism, turnover, proliferation, as well as type I interferon and
255 TNF signaling. Unlike in CD4, CD14, or B cells, NK cells do not experience as significant
256 upregulation of interferon or JAK/STAT pathways. Interestingly, many inflammatory pathways
257 in NK cells are downregulated in SCLE and lupus panniculitis, suggesting a potential regulatory
258 role of NK cells in these subtypes, and that downregulation of inflammatory pathways in NK

259 cells could be related to these phenotypes. NK cells exhibit few differentially upregulated
260 pathways for patients with malar rash and photosensitivity.
261
262 **Cell-type enrichment in cutaneous disease states in SLE**
263 Finally, after defining cell-type specific and globally dysregulated pathway fingerprints
264 for each lupus-related rash, we then asked the question whether we could detect significant
265 relative differences in the cell-type enrichment in the blood of patients with specific lupus-
266 related rashes. We conducted cell type enrichment analysis using XCell (28) on the bulk
267 transcriptome of whole blood from the same cohort. We identified a total of 17 immune cell
268 types in the blood that had significant enrichment in the SLE cohort, including CD4 naïve and
269 memory T cells, naïve and memory B cells, naïve and memory CD8+ T cells, monocytes,
270 neutrophils, and plasma cells. The strongest normalized cell type enrichments signatures were
271 seen in the CD4+ memory and naive T cells, naïve and memory CD8+ T cells, monocytes, B cells
272 (Figure 5A). Larger positive values indicate a higher enrichment score. For several rashes, we
273 identified statistically significant changes (padj < 0.05) in the cell type enrichment in the blood,
274 including discoid lupus, mucosal ulcers, alopecia, and in photosensitivity (Figure 5B-E). There
275 was an increase in class-switched memory B cells and in plasma cells in patients with mucosal
276 ulcers (Figure 5C). In alopecia and in photosensitivity, there was a decrease in relative
277 enrichment score in CD8+ naive T cells, suggesting an immunoregulatory role for this cell type
278 in those rashes. In contrast, there was a corresponding increase in enrichment of CD4+ T cells
279 for alopecia and photosensitivity (Figure 5B, D). In discoid lupus, there was strong relative
280 increases in enrichment score for B cells in the blood, including both naive and memory B cells

281 (Figure 5E). All other comparisons of cell type enrichment in the global blood compartment
282 were not significant.
283
284 **Discussion**
285 This study provides a comprehensive, large-scale transcriptomic analysis of cutaneous
286 phenotypes from a longitudinal cohort of systemic lupus erythematosus (SLE) patients, allowing
287 us to identify key molecular pathways involved in specific skin-related manifestations of lupus.
288 By utilizing both whole blood bulk RNA sequencing and immune cell-sorted RNA sequencing
289 data from the CLUES cohort, we have successfully mapped unique molecular correlates
290 associated with 10 different rashes observed in SLE patients. We conducted parallel analyses of
291 bulk RNAseq and cell-sorted RNAseq data, which allowed for a more refined understanding of
292 immune cell contributions to cutaneous manifestations in SLE. The integration of these datasets
293 allowed us to construct an interactome network by overlapping differentially expressed genes
294 across various cutaneous manifestations of SLE. This network analysis highlighted shared
295 pathways between rash subtypes, contributing to a deeper understanding of the molecular
296 underpinnings of these manifestations. Hallmark pathway analysis of both unsorted and cell-
297 sorted data identified distinct molecular pathway "fingerprints" for different rashes, providing
298 critical insight into the immune and molecular mechanisms underlying these skin findings. Cell-
299 type-specific findings further illuminate the cellular contributors to specific cutaneous
300 phenotypes. Our results have direct therapeutic implications for patients that suffer from
301 specific cutaneous phenotypes of SLE.

302 One key unexpected finding from our analysis was that the type I interferon (IFN-α)
303 pathway, known as a defining hallmark of lupus disease activity and pathogenesis, is not
304 universally upregulated across all cutaneous subtypes, suggesting that targeting IFN-α may be
305 more effective in certain lupus subtypes compared to others. We found that IFN-α and IFN-
306 gamma pathways were upregulated in patients with acute cutaneous lupus (malar rash),
307 discoid lupus, SCLE, alopecia, livedo reticularis, and lupus panniculitis. In contrast, patients with
308 skin ulcers and mucosal ulcers did not have significant upregulation of interferon pathways.
309 This absence of IFN signaling in certain cutaneous phenotypes suggests that SLE skin
310 manifestations may involve different immunological pathways, underscoring the heterogeneity
311 of the disease. This also represents a potential targetable therapeutic opportunity for patients
312 with refractory lupus cutaneous phenotypes that tend to have stronger type I IFN signatures.
313 This suggests that anifrolumab (Saphnelo), a biologic medication targeting IFN-α which is
314 approved in the US for moderate to severe SLE, is a potential treatment for refractory
315 cutaneous lupus in patients with SLE.
316 Subacute cutaneous lupus erythematosus is a cutaneous subtype of lupus that is also
317 poorly understood. Our findings show that patients with SCLE exhibited a broad and strong
318 upregulation of several cytokine immune pathways, including IFN-α, IFN-γ, TNF-α, IL2-STAT5
319 signaling, and IL6-JAK-STAT3 signaling particularly in B cells and CD4 T cells. The involvement of
320 both IFN and multiple JAK-related pathways in specific immune cell types suggests that SCLE
321 patients with SLE may benefit from treatment with JAK inhibitors as well as type I interferon
322 blockade. The other cutaneous phenotypes that had strong upregulation of JAK pathways were
323 in discoid lupus erythematosus and acute cutaneous lupus. These findings is particularly

324 noteworthy given the emerging role of JAK inhibitors in autoimmune diseases. Several FDA
325 approved JAK inhibitors include topical (ruxolitinib) and systemic (upadacitinib and abrocitinib)
326 formulations, which are being used for vitiligo and atopic dermatitis, respectively. Our findings
327 provide a direct rationale for investigating either systemic or topical JAK inhibitors as a
328 potential treatment for SCLE and discoid lupus in a real-world clinical trial.

329 CD4 T cells are known to play a central in the pathogenesis of SLE (29, 30), but the role
330 of specific pathways dysregulated in the blood compartment related to skin manifestations are
331 not well studied. From our cell-type specific analysis, we identified significant enrichment of
332 differentially expressed genes in CD4 T cells and B cells, suggesting a prominent role of these
333 immune cells in the pathophysiology of both SCLE and livedo reticularis. SCLE and livedo
334 reticularis shared many common upregulated genes in the CD4 T cell compartment, further
335 highlighting the importance of T-cell specific responses in these rashes. Similarly, our study
336 identifies specific pathways involved in UV response that are shared by SCLE and
337 photosensitivity, indicating a potential unexpected role of CD14+ monocytes in the
338 pathophysiology of photosensitivity in lupus.

339 We also identified that alopecia in SLE patients, which is a common and psychosocially
340 distressing phenotype, was associated with upregulation of heme metabolism pathways. Iron
341 deficiency has been known to be linked to hair loss conditions such as androgenetic alopecia.
342 This observation suggests that therapeutic strategies aimed at addressing iron metabolism,
343 especially in patients with anemia, may be beneficial in treating lupus-related alopecia.
344 Surprisingly, mucosal ulceration, alopecia, and livedo reticularis were associated with
345 upregulation of inflammatory programs in NK cells, suggesting that NK cells may play an

346 underappreciated role in the pathogenesis of these cutaneous manifestations. Cell type
347 enrichment analysis further predicted differential enrichment of specific immune cell types in
348 various cutaneous manifestations of SLE, including malar rash, discoid rash, SCLE, alopecia, and
349 photosensitivity. These findings suggest that different immune cells may be preferentially
350 involved in the development of distinct rashes, further supporting the notion of immune
351 heterogeneity in SLE.

352 A strength of this study is the robust cohort of SLE patients and the availability of high-
353 quality large-scale transcriptomic data, which allows us to obtain significant insights into the
354 molecular basis of lupus-related cutaneous manifestations. The CLUES cohort is one of the
355 largest SLE cohorts in the world with significant genetic and ethnic diversity and rich
356 phenotyping data. Furthermore, parallel use of bulk RNAseq and immune cell-sorted RNAseq
357 data allows for a deeper understanding of the specific immune cells contributing to different
358 rash subtypes. Pathway and interactome analysis identified shared and unique molecular
359 pathways, with potential therapeutic targets, such as JAK inhibitors for SCLE. We also
360 discovered unexpected roles for CD14+ monocytes in photosensitivity and NK cells in alopecia,
361 mucosal ulceration, and livedo reticularis, which identifies new avenues for therapeutic
362 development. A weakness of this study is the use of bulk RNAseq data from whole blood, which
363 may not fully capture the complexity of local immune responses at the site of the skin rash. At
364 the same time, the use of bulk RNAseq allows us to quickly profile several hundred patients at
365 once across a large cohort, since conducting scRNAseq across such as large cohort is very costly.
366 Furthermore, scRNAseq can be biased toward immune cell types that are more abundant in
367 these patients, and are typically only done on PBMCs, ignoring contributions from other

368 important cell types such as the granulocytes of the myeloid compartment. Although the study
369 investigates blood immune signatures across multiple cutaneous subtypes, it does not
370 incorporate skin biopsy samples at the time of blood transcriptomics to directly assess the
371 immune responses within affected tissues, which could provide additional valuable insights. At
372 the same time, the goal of the study was to identify molecular signatures from whole blood
373 that are predictive of rashes without requiring a skin biopsy, which can only be done on active
374 lesional skin. While our findings support potential therapeutic targets and modalities, including
375 JAK inhibitors, further clinical validation and functional studies are required to confirm the
376 efficacy and safety of these treatments in specific subgroups of SLE patients, including those
377 with low disease burdens. The cohort size and demographic characteristics may limit the
378 generalizability of the findings, requiring replication in larger, more diverse populations to
379 confirm the observed molecular pathways and immune cell signatures. One limitation of this
380 study is related to recruitment primarily patients with SLE disease without matched controls. As
381 a result, the objective of this study was to identify molecular markers that could be used to
382 predict cutaneous phenotypes among a cohort with known SLE disease, rather than
383 differentiate SLE patients from controls. Another limitation of this study is that a subset of
384 patients in this cohort had historical manifestations of cutaneous lupus that may or may not be
385 flaring or active at time of clinical sampling. We recognize that all clinical manifestations of
386 lupus are not fixed, and dynamic fluctuation of disease activity is characteristic of autoimmune
387 inflammatory conditions.

388 Taken together, our conclusions represent a significant step forward in understanding
389 the molecular pathways and immune cell involvement in SLE-related skin manifestations,

390 spanning both common and rare phenotypes. The identification of pathway "fingerprints" and
391 novel therapeutic targets holds promise for the development of more personalized and
392 effective treatments for SLE patients, particularly those with specific cutaneous manifestations,
393 and may allow us to predict which patients may benefit from specific therapies to advance
394 personalized medicine for SLE.
395
396 **Materials and Methods**
397
398 **Study design**
399 Participants were recruited from the California Lupus Epidemiology Study (CLUES) as
400 outlined previously (*15*). CLUES was approved by the Institutional Review Board of the
401 University of California, San Francisco. All participants signed a written informed consent to
402 participate in the study. Study procedures involved an in-person research clinic visit, which
403 included collection and review of medical records prior to the visit; history and physical
404 examination conducted by a physician specializing in lupus; a collection of biospecimens,
405 including peripheral blood for clinical and research purposes; and completion of a structured
406 interview administered by an experienced research assistant. During the interview,
407 comprehensive clinical characteristics were documented including overall disease activity
408 (Systemic Lupus Erythematosus Disease Activity Index score (SLEDAI) and lupus severity index),
409 medications, self-reported race/ethnicity, sex, and specific cutaneous manifestations related to
410 SLE. All SLE diagnoses were confirmed by board-certified study physicians based upon one of
411 the following definitions: (a) meeting ≥4 of the 11 American College of Rheumatology (ACR)

412 revised criteria for the classification of SLE as defined in 1982 and updated in 1997, (b) meeting
413 3 of the 11 ACR criteria plus a documented rheumatologist's diagnosis of SLE, or (c) a confirmed
414 diagnosis of lupus nephritis, defined as fulfilling the ACR renal classification criterion (>0.5
415 grams of proteinuria per day or 3+ protein on urine dipstick analysis) or having evidence of
416 lupus nephritis on kidney biopsy. Included in this data collection were cutaneous manifestations
417 of lupus. In this study, we focused on a subset of 10 different rashes and/or cutaneous
418 manifestations related to SLE: acute cutaneous lupus (malar rash), discoid lupus (DLE),
419 photosensitivity, mucosal ulcers, skin ulcers, alopecia, subacute cutaneous lupus (SCLE), lupus
420 panniculitis, livedo reticularis, and other rashes related to SLE. We focused the analysis on skin
421 phenotypes that appeared in at least 10 patients within the entire cohort. Clinical phenotypes
422 that were excluded from our analysis due to low incidence include bullous lupus
423 erythematosus, calcinosis cutis, lupus perniosis, and sclerodactyly. All clinical data collected at
424 sampling and the self-reported race was used for downstream analyses.
425
426 **RNA-seq processing and quality control**
427 The two datasets utilized in this study includes bulk RNA sequencing data from whole
428 blood and cell-sorted peripheral blood mononuclear cells from the CLUES cohort. Whole blood
429 was collected from patients into PAXgene tubes and underwent human rRNA and globin RNA
430 depletion followed by library preparation using the NEBNext library preparation kit. Paired end
431 Illumina sequencing was then carried out on a Novaseq6000. Host gene counts were generated
432 by pseudoalignment against the human transcriptome using Kallisto (31). Adapter-trimmed
433 reads were used as input. We quantified gene expression using raw counts and kept the genes

434 that showed an average FPKM value across the samples >0.5. FastQC (v0.11.8) was run to
435 assess the quality of the sequence reads. For the sequencing on sorted immune cells, samples
436 were isolated from patient donors as outlined previously (16). Cells were isolated from
437 peripheral blood utilizing magnetic beads (CD14+ monocytes, B cells, CD4+ T cells, and NK cells)
438 using EasySep protocol from STEM cell technologies on 120 patients totaling 480 samples. RNA
439 was extracted using a Qiagen column and quality was assessed on Agilent bioanalyzer. Libraries
440 were sequenced on HiSeq4000 PE150. Salmon v0.8.2 (32) was used for our alignment-free
441 pipeline. Adapter-trimmed reads were used as input. We quantified gene expression using raw
442 counts and kept the genes that showed an average FPKM value across the samples >0.5. FastQC
443 (v0.11.8) was run to assess the quality of the sequence reads. Genes with low expression were
444 filtered out before statistical testing. The cell sorted data is deposited and publicly available on
445 the Gene Expression Omnibus (GEO) website under the accession GSE164457. The other data is
446 available on request from the authors.
447
448 **Differential expression and pathway analyses**
449 We performed differential expression gene testing with DESeq2 (v.1.24.0 R package)
450 (*19*) using default settings. Sequence lane, medication at time of sampling, sex, batch/plate,
451 and race were entered as covariates within the DESeq2 model using a negative
452 binomial generalized linear model. We conducted differential expression by comparing patients
453 with and without specific cutaneous clinical manifestations of SLE. For example, we conducted
454 differential expression analysis for malar rash using DESeq2 by comparing patients with and
455 without malar rash, with patients without malar rash as the reference baseline. Similarly, we

456 conducted differential expression analysis on the cell-sorted bulk RNAseq dataset (CD4, CD14,
457 CD19, NK cell) in the same manner. Statistical significance was set a 5% FDR (Benjamini-
458 Hochberg). Differential expression analysis was conducted for all 10 cutaneous phenotypes that
459 had at least 10 patients exhibiting the phenotype. For pathway analyses to identify immune
460 pathways and signatures associated with each cutaneous phenotype, we inputted the sorted
461 differentially expressed gene lists defining the log 2 fold change and the adjusted p-values into
462 the Bioconductor package fgsea (v 1.10.1) for gene set enrichment analysis (GSEA) (*20*) with
463 Hallmark pathways taken from the MSigDB (26).
464
465 **Cell type enrichment analyses**
466 The XCell package was used to carry out cell type enrichment analyses (28). This was
467 conducted on the merged and normalized bulk RNAseq data for the entire cohort. XCell
468 performs cell type enrichment analysis from gene expression for 64 immune and stroma cell
469 types, based on transcriptomic signatures from thousands of pure cell types from various
470 sources as outlined previously (28). The existing compendium of cell type signatures were
471 filtered to remove cell types not relevant to this analysis. The false discovery rate was
472 controlled by the Benjamini–Hochberg method.
473
474 **Statistics and reproducibility**
475 The statistical analyses for each part of the approach are described above. A threshold of P =
476 0.05 for false discovery rate and for adjusted P-values was set. The code is publicly
477 available to ensure the reproducibility of our results.

478

479 **Supplementary Materials**

480 Fig. S1-S6 for supplementary figures.

481 Figure S1: CLUES cohort demographic histograms.

482 Figure S2: Quality control of whole blood bulk RNAseq

483 Figure S3: Principal component plot of whole blood bulk transcriptome and additional clinical

484 characteristics

485 Figure S4: Hierarchical clustering of clinical characteristic, highlighting clinical subtypes of SLE-

486 related rashes

487 Figure S5: Upset plots on overlapping differentially expressed genes for SLE rash subtypes

488 Figure S6: Pathway enrichment plots from gene set enrichment analysis of whole blood bulk

489 RNAseq for each SLE rash subtype

490

491 **Acknowledgments:** We are grateful to all patients who participated in this study. We would like

492 to thank the administrative and medical team of UCSF Rheumatology clinics. We would like to

493 thank the PREMIER center as well as members of the Sirota Lab for useful discussion.

494

495 **Funding**

496 EYL is supported by National Institutes of Health grant T32AR007175, a Dermatology

497 Foundation Dermatologist Investigator Research Fellowship, a Dermatology Foundation

498 Physician-Scientist Career Development Award, and a Hidradenitis Suppurativa Foundation

499 Translational Research Grant. MS is supported by grants from the Rheumatology Research

Foundation and a the P30-AR070155 grant from the National Institutes of Health, National Institute of Arthritis and Musculoskeletal and Skin Diseases (NIAMS). This work was funded by a grant from the Centers for Disease Control and Prevention of the U.S. Department of Health and Human Services (5U01DP006486).

Author contributions: All authors were involved in drafting the article or revising it critically for important intellectual content, and all authors approved the final version to be published. EYL and MS had full access to all the data in the study and take responsibility for the integrity of the data and the accuracy of the data analysis.

Competing interests: Authors declare that they have no competing interests.

Data and materials availability

The data that support the findings of this study are available from the corresponding author upon reasonable request.

516 **Figures:**

517

518 **Figure 1: Study overview and design.** Patients were recruited from the CLUES cohort and bulk

519 RNA sequencing was conducted. Data was processed for transcriptome quantification and

520 quality control. We then associated clinical parameters with cutaneous manifestations of SLE,

521 and downstream conducted differential gene expression analysis, pathway analysis, and cell

522 type enrichment analysis.

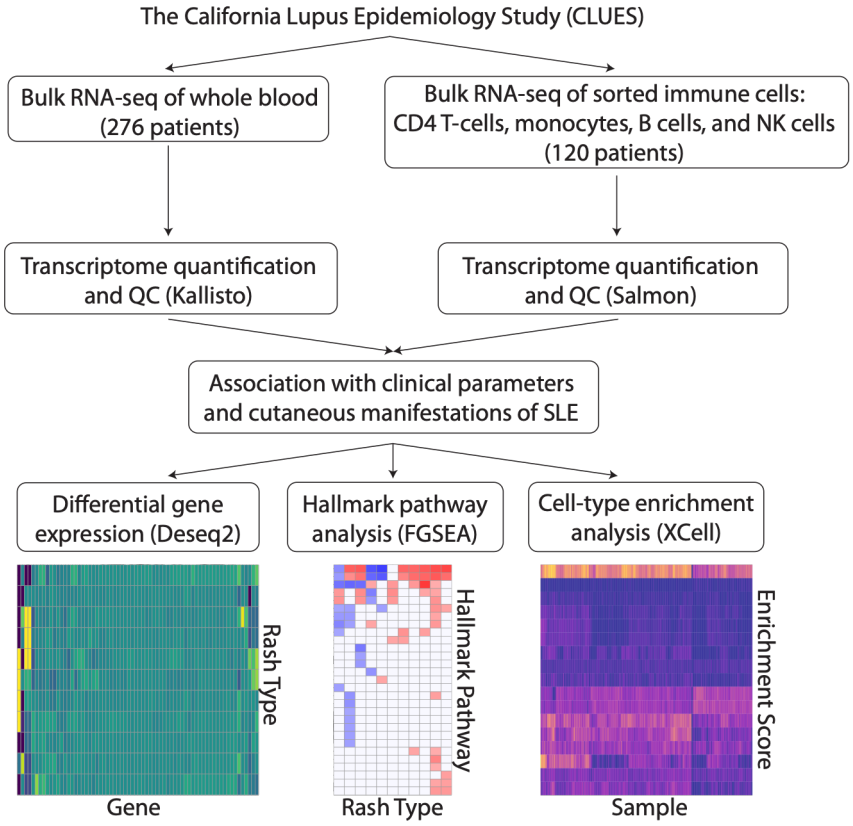

523

524

525 **Figure 2: Transcriptomic landscape of cutaneous manifestations of SLE in the CLUES cohort**.

526 (A) Clinical characteristics and cutaneous subtypes of lupus across the entire cohort. (B) PCA

527 plots showing whole blood bulk RNAseq and each associated SLE-related rash subtype.

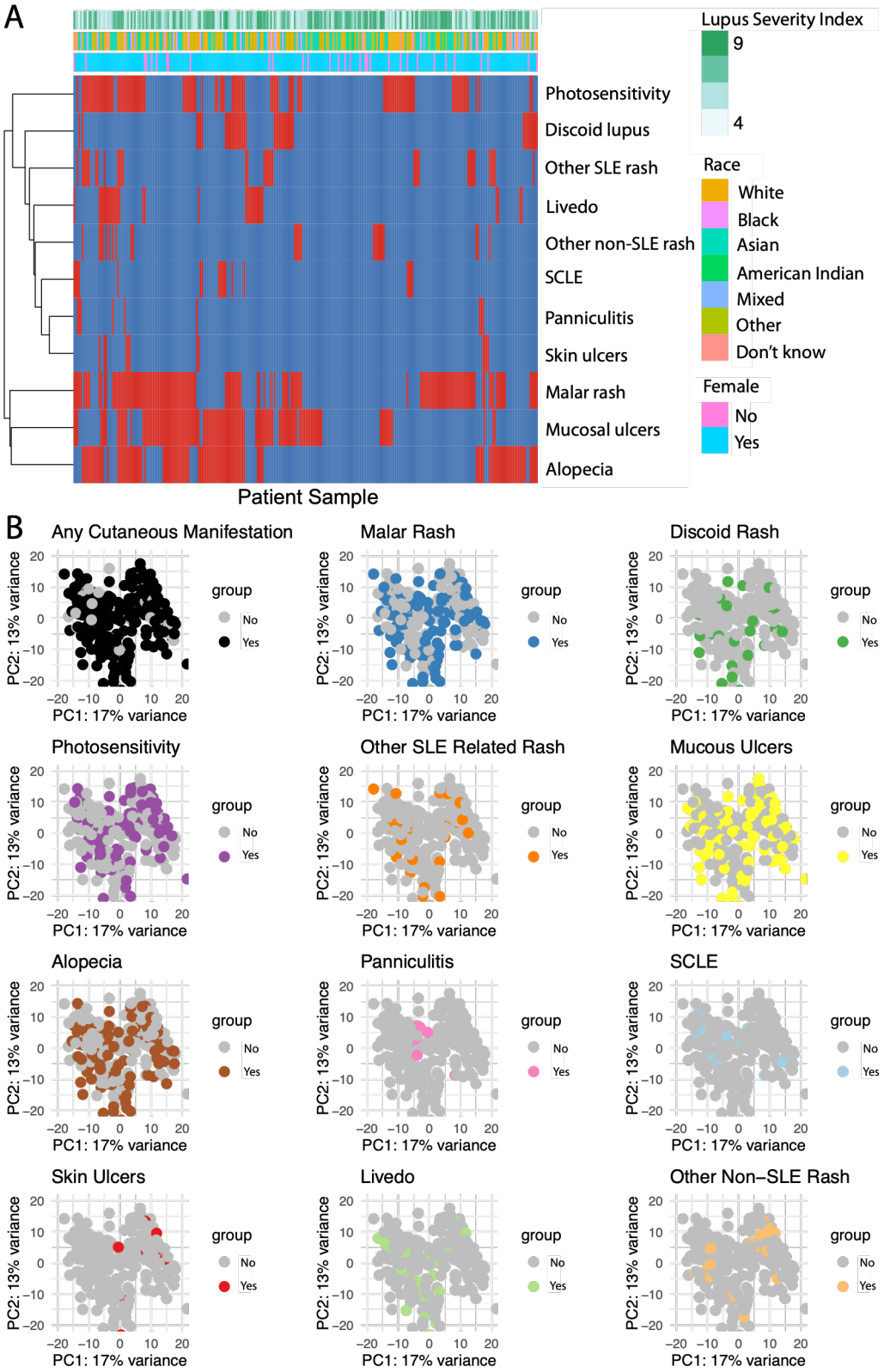

528

529 **Table 1: CLUES cohort demographic characteristics**

Characteristics	Overall (N = 276)
Sex	
Female	244 (88.4%)
Male	32 (11.6%)
Age	44.5 ± 14.0 years
Race	
White	99
Black	29
Asian	102
American Indian	1
Mixed	10
Other	32
Unknown race	3
Lupus severity index	6.9 ± 1.6
Malar rash	139 (50.0%)
Discoid rash	40 (14.4%)
Photosensitivity	103 (37.3%)
Mucosal ulcers	120 (43.5%)
Alopecia	110 (39.9%)
Panniculitis	9 (3.3%)
SCLE	18 (6.5%)

Skin Ulcers	12 (4.3%)
Livedo reticularis	32 (11.6%)
Other SLE related rash	35 (12.7%)
Other Non-SLE rash	25 (9.1%)

530

531

532 **Figure 3**: **Interactome and disease signatures of distinct SLE-related rashes**. Differential gene
533 expression analysis identified interactome and disease signatures of each distinct SLE rash
534 subtype, shown for whole blood (A), and in immune cell-sorted data for CD4 T cells (B), CD14
535 monocytes (C), CD19 B cells (D), and NK cells (E). Networks of each cutaneous manifestation is
536 constructed based on number of differentially expressed genes in common. Edge thickness is
537 directly proportional to the number of overlapping differentially expressed genes in common
538 between clinical manifestations. Heatmaps show upregulated (yellow) and downregulated
539 (blue) differentially expressed genes by log2-fold-change taken from the union of all
540 differentially expressed genes across cutaneous phenotypes.

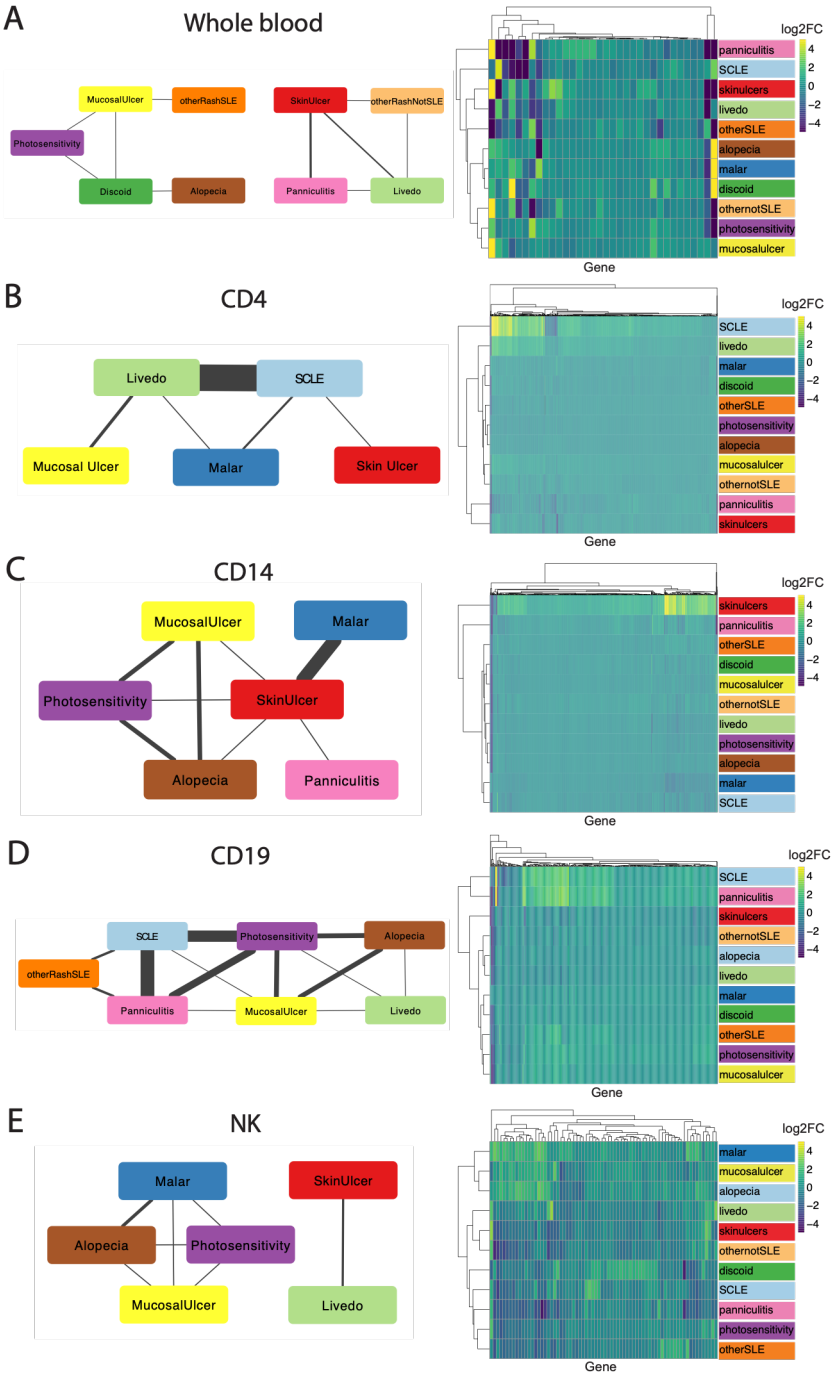

541

542 **Table 2**: **Differentially expressed genes by SLE cutaneous phenotype type in whole blood and**

543 **immune cell sorted data.**

544

Clinical Feature	Whole blood	CD4 (T cell)	CD14 (monocyte)	CD19 (B cell)	NK cell
Malar	1	58	16	0	20
Discoid	2	1	1	0	18
Photosensitivity	2	1	6	198	5
Other rash SLE	6	1	0	4	6
Mucosal ulcers	4	5	7	16	5
Alopecia	6	0	7	7	19
Panniculitis	8	2	6	85	0
SCLE	4	737	0	178	4
Skin ulcers	6	5	572	2	2
Livedo	2	258	1	1	5
Other rash	2	0	0	0	0

545

546 **Figure 4**: **Unsupervised clustering of signaling pathways defining cutaneous manifestations of**

547 **SLE.** Unsupervised hierarchical clustering of normalized enrichment scores for biological

548 pathways from GSEA of bulk RNAseq data from whole blood (A), CD4+ T cells (B), CD14+

549 monocytes (C), CD19+ B cells (D), or NK cells (E). Only significant (FDR < 0.05) upregulated (red)

550 or downregulated (blue) pathways are shown.

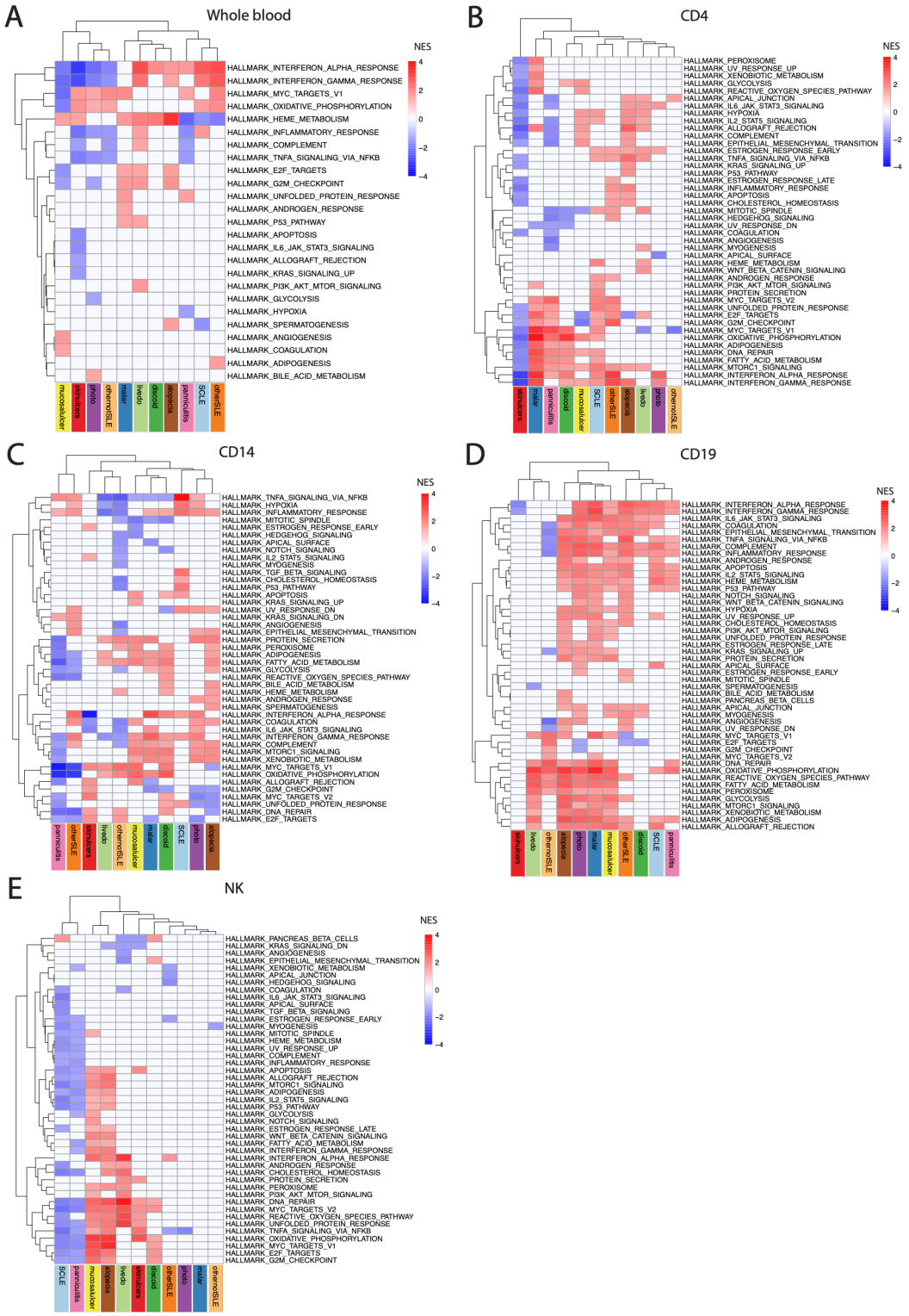

Figure 5: Cell type enrichment in cutaneous disease states in SLE. (A) Cell type enrichment calculated with XCell from bulk RNAseq from all CLUES patients (N = 276), with normalized

554 abundances for each predicted cell type. Significant differences (padj < 0.05) were detected in
555 enrichment scores for CD4+ and CD8+ T cells for patients with photosensitivity (B), in memory B
556 cells and plasma cells for patients with mucosal ulcers (C), and in CD4+ and naive CD8+ T cells
557 for patients with alopecia (D). Significant differences were also observed in enrichment of B
558 cells including naive and memory B cells in discoid lupus (E).

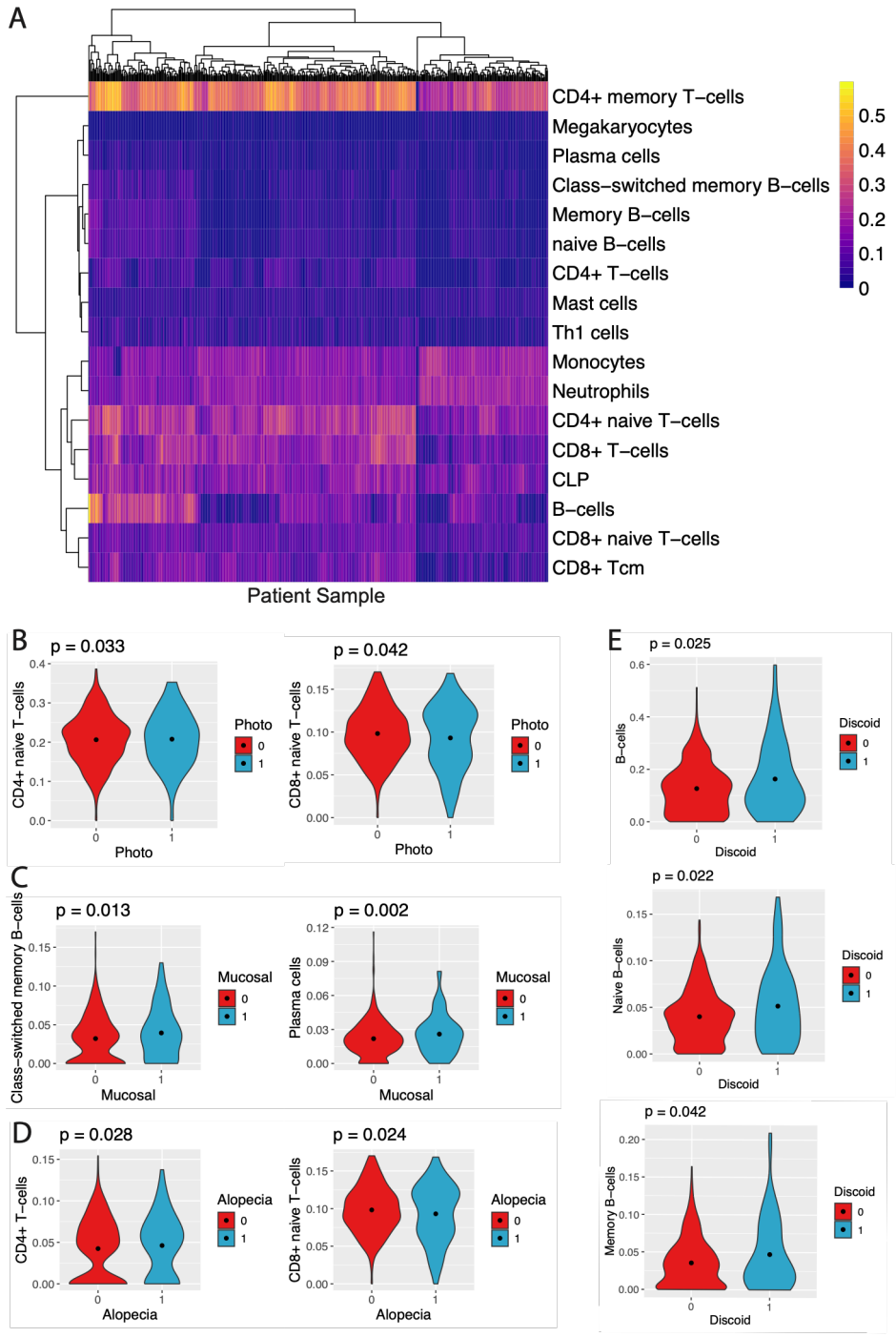
A
CD4+ memory T−cells
Megakaryocytes
Plasma cells
Class−switched memory B−cells
Memory B−cells
naive B−cells
CD4+ T−cells
Mast cells
Th1 cells
Monocytes
Neutrophils
CD4+ naive T−cells
CD8+ T−cells
CLP
B−cells
CD8+ naive T−cells
CD8+ Tcm
Patient Sample
0.5
0.4
0.3
0.2
0.1
0
B
p = 0.033
CD4+ naive T−cells
Photo
p = 0.042
CD8+ naive T−cells
Photo
C
p = 0.013
Class−switched memory B−cells
Mucosal
p = 0.002
Plasma cells
Mucosal
D
p = 0.028
CD4+ T−cells
Alopecia
p = 0.024
CD8+ naive T−cells
Alopecia
E
p = 0.025
B−cells
Discoid
p = 0.022
Naive B−cells
Discoid
p = 0.042
Memory B−cells
Discoid

559

560

561 **References:**

562

563 1. Tsokos GC. Systemic Lupus Erythematosus. *N Engl J Med*. 2011;365(22):2110–2121.

564 2. Uva L, et al. Cutaneous Manifestations of Systemic Lupus Erythematosus. *Autoimmune Dis*.
565 2012;2012(1):834291.

566 3. YELL JA, MBUAGBAW J, BURGE SM. Cutaneous manifestations of systemic lupus
567 erythematosus. *Br J Dermatol*. 1996;135(3):355–362.

568 4. Wieczorek IT, et al. Systemic Symptoms in the Progression of Cutaneous to Systemic Lupus
569 Erythematosus. *JAMA Dermatol*. 2014;150(3):291–296.

570 5. Werth VP. Clinical manifestations of cutaneous lupus erythematosus. *Autoimmun Rev*.
571 2005;4(5):296–302.

572 6. Jia BB, et al. Emerging Techniques in Spatial Multiomics: Fundamental Principles and
573 Applications to Dermatology. *J Investig Dermatol*. [published online ahead of print: 2024].
574 https://doi.org/10.1016/j.jid.2024.09.006.

575 7. Nehar-Belaid D, et al. Mapping systemic lupus erythematosus heterogeneity at the single-cell
576 level. *Nat Immunol*. 2020;21(9):1094–1106.

577 8. Nakano M, et al. Distinct transcriptome architectures underlying lupus establishment and
578 exacerbation. *Cell*. 2022;185(18):3375-3389.e21.

579 9. Der E, et al. Single cell RNA sequencing to dissect the molecular heterogeneity in lupus
580 nephritis. *JCI Insight*. 2017;2(9):e93009.

581 10. Seremet T, et al. Immune modules to guide diagnosis and personalized treatment of
582 inflammatory skin diseases. *Nat Commun*. 2024;15(1):10688.

583 11. Liu Y, et al. Classification of human chronic inflammatory skin disease based on single-cell
584 immune profiling. *Sci Immunol*. 2022;7(70):eabl9165.

585 12. Perez RK, et al. Single-cell RNA-seq reveals cell type–specific molecular and genetic
586 associations to lupus. *Science*. 2022;376(6589):eabf1970.

587 13. Panousis NI, et al. Combined genetic and transcriptome analysis of patients with SLE:
588 distinct, targetable signatures for susceptibility and severity. *Ann Rheum Dis*.
589 2019;78(8):annrheumdis-2018-214379.

590 14. Bennett L, et al. Interferon and Granulopoiesis Signatures in Systemic Lupus Erythematosus
591 Blood. *J Exp Med*. 2003;197(6):711–723.

592 15. Banchereau R, et al. Personalized Immunomonitoring Uncovers Molecular Networks that
593 Stratify Lupus Patients. *Cell*. 2016;165(3):551–565.

594 16. Lanata CM, et al. A phenotypic and genomics approach in a multi-ethnic cohort to subtype
595 systemic lupus erythematosus. *Nat Commun*. 2019;10(1):3902.

596 17. Lanata CM, et al. Dynamics of Methylation of CpG Sites Associated With Systemic Lupus
597 Erythematosus Subtypes in a Longitudinal Cohort. *Arthritis Rheumatol (Hoboken, Nj)*.
598 2022;74(10):1676–1686.

599 18. Andreoletti G, et al. Transcriptomic analysis of immune cells in a multi-ethnic cohort of
600 systemic lupus erythematosus patients identifies ethnicity- and disease-specific expression
601 signatures. *Commun Biol*. 2021;4(1):488.

602 19. Cutts Z, et al. Cell-Specific Transposable Element and Gene Expression Analysis Across
603 Systemic Lupus Erythematosus Phenotypes. *ACR Open Rheumatol*. [published online ahead of
604 print: 2024]. https://doi.org/10.1002/acr2.11713.

605 20. Billi AC, et al. Nonlesional lupus skin contributes to inflammatory education of myeloid cells
606 and primes for cutaneous inflammation. *Sci Transl Med*. 2022;14(642):eabn2263.

607 21. Zheng M, et al. Single-cell sequencing shows cellular heterogeneity of cutaneous lesions in
608 lupus erythematosus. *Nat Commun*. 2022;13(1):7489.

609 22. Zheng M, et al. Single-cell transcriptome reveals immunopathological cell composition of
610 skin lesions in subacute cutaneous lupus erythematosus. *Clin Immunol*. 2022;245:109172.

611 23. Farkas L, et al. Plasmacytoid Dendritic Cells (Natural Interferon- α/β-Producing Cells)
612 Accumulate in Cutaneous Lupus Erythematosus Lesions. *Am J Pathol*. 2001;159(1):237–243.

613 24. Love MI, Huber W, Anders S. Moderated estimation of fold change and dispersion for RNA-
614 seq data with DESeq2. *Genome Biol*. 2014;15(12):550.

615 25. Subramanian A, et al. Gene set enrichment analysis: A knowledge-based approach for
616 interpreting genome-wide expression profiles. *Proc Natl Acad Sci*. 2005;102(43):15545–15550.

617 26. Liberzon A, et al. The Molecular Signatures Database Hallmark Gene Set Collection. *Cell Syst*.
618 2015;1(6):417–425.

619 27. Katsiari CG, Liossis S-NC, Sfikakis PP. The Pathophysiologic Role of Monocytes and
620 Macrophages in Systemic Lupus Erythematosus: A Reappraisal. *Semin Arthritis Rheum*.
621 2010;39(6):491–503.

622 28. Aran D, Hu Z, Butte AJ. xCell: digitally portraying the tissue cellular heterogeneity landscape.
623 *Genome Biol*. 2017;18(1):220.

624 29. Suárez-Fueyo A, Bradley SJ, Tsokos GC. T cells in Systemic Lupus Erythematosus. *Curr Opin*
625 *Immunol*. 2016;43:32–38.

626 30. Li H, et al. Abnormalities of T cells in systemic lupus erythematosus: new insights in
627 pathogenesis and therapeutic strategies. *J Autoimmun*. 2022;132:102870.

628 31. Bray NL, et al. Near-optimal probabilistic RNA-seq quantification. *Nat Biotechnol*.
629 2016;34(5):525–527.

630 32. Patro R, et al. Salmon provides fast and bias-aware quantification of transcript expression.
631 *Nat Methods*. 2017;14(4):417–419.

632